Kwan, J.S.H., Chan, S.L., Cheuk, J.C.Y. and Koo, R.C.H. (2014) A case study on an open hillside landslide impacting on a flexible rockfall barrier at Jordan Valley, Hong Kong. Landslides, Springer-Verlag Berlin Heidelerg, Vol 11, pp1037-1050

The Assessment Board selected this paper for the 2016 HKIE Geotechnical Paper Award, for its potential to advance local geotechnical practice and its quality of writing for the readership of practicing geotechnical engineers. It hence noted:

> The paper Kwan et al (2014) documented in detail the first local case of response of a flexible barrier to open hillside landslide debris. It reviewed succinctly the state of the art of flexible barrier design to support a back-analysis. Observations on improving local practice were put forward. Although flexible barrier design technology has since advanced significantly, most of the paper's observations remain relevant and the paper provides a faithful record of its time and a milestone against which the rapid progress of technology could be visualized. The detailed record could be used to calibrate newer design technology. The paper is carefully structured and amply illustrated to bring the subject to readers of a wide range of background knowledge.

Kwan, J.S.H., Chan, S.L., Cheuk, J.C.Y. and Koo, R.C.H. (2014). A case study on an open hillside landslide impacting on a flexible rockfall barrier at Jordan Valley, Hong Kong. Landslides, December 2014, Vol. 11, Issue 6, pp. 1037-1050

The final publication is available at Springer via http://dx.doi.org/10.1007/s10346-013-0461-x

A case study on an open hillside landslide impacting on a flexible rockfall barrier at Jordan Valley, Hong Kong

Kwan, J.S.H., Chan, S.L., Cheuk, J.C.Y. and Koo, R.C.H.

Abstract: A case study on an open hillside landslide impacting on a flexible rockfall barrier at Jordan Valley, Hong Kong is presented in this paper. The landslide occurred sometime in June 2008. This is so far the only case history of landslide debris having been intercepted by a flexible rockfall barrier in Hong Kong. The landslide scar is 10 m wide and 7 m long, and the landslide volume is about 110 m^3. The landslide debris was largely retained by the barrier but two of the barrier posts were severely damaged and failed. Debris mobility analysis and structural analysis of this case history have been undertaken with a view to obtaining a better understanding of the possible landslide dynamics and behaviour of flexible barrier upon debris impact. The analyses appear to have reproduced some of the salient field observations. The probable key contributory factors to the failure are highlighted and discussed. Through the study, the possible range of equivalent pseudo-static impact pressure exerted on the flexible barrier by the landslide debris is assessed. The site observations and results of the analyses provide insights pertaining to the importance of robustness in the design and detailing of flexible debris-resisting barriers.

Keywords: open hillside landslide, Jordan Valley, flexible rockfall barrier, flexible debris-resisting barriers

1. INTRODUCTION

Flexible barriers have been commonly used for rockfall mitigation. Their use is a highly attractive option of landslide risk mitigation measure for natural terrain, as it is less visually intrusive compared to rigid barriers (e.g. concrete check dams). Flexible barriers also have the advantage of relatively easy construction, since the barriers are usually made of fairly light-weight materials. Over the past years, flexible rockfall barriers have occasionally been hit by debris flows and landslide debris in different countries. A number of field cases and physical tests have demonstrated that flexible barriers could be capable of arresting a certain amount of debris (Roth et al, 2004; Duffy, 1998). However, detailed analyses of the case histories are limited to date.

An open hillside landslide in Jordan Valley, Hong Kong was reported to the Geotechnical Engineering Office (GEO) of Hong Kong Special Administrative Region Government in December 2009. A subsequent aerial photograph study suggested that the landslide could have occurred during a heavy rainstorm in June 2008. Ground mass of about 110 m^3 in volume detached from a natural hillside in the form of an open hillside landslide. It consists of matrix-supported debris mixed with rounded to sub-rounded boulders and vegetation. Its thickness increases towards the frontal end from the rear end of deposition. Also, boreholes were sunk at the site for design of site formation works. The soil descriptions given in the borehole logs are silty, fine to coarse sand with some angular to subangular, fine to medium gravel sized quartz and granite fragments. The landslide debris struck a flexible rockfall barrier installed at the toe of the hillside of Jordan Valley. The flexible barrier, which comprised an assembly of steel posts, netting, steel cable ropes, energy dissipaters, etc, was a proprietary product originally installed to mitigate boulder falls from the hillside. So far, this is the only case history of flexible barrier intercepting landslide debris in Hong Kong. A thorough study, comprising field inspections and numerical analyses, of the Jordan Valley landslide impacting on the flexible barrier has been carried out with a view to deriving insights that are pertinent to the design and detailing of flexible debris-resisting barriers.

2. PREVIOUS WORK ON THE DEVELOPMENT AND DESIGN OF FLEXIBLE DEBRIS-RESISTING BARRIERS

Flexible rockfall barriers have been found to have successfully arrested and contained landslide debris in different site settings. Duffy (1998) reported several of these cases where flexible barriers were used to protect highways in the USA. For example, barriers installed along Highway 41 in California retained some 60 m^3 of debris of rain-induced failure of a hillside. In order to study the potential application of flexible barriers in resisting landslide debris, six large-scale flume tests of flexible barriers intercepting landslide debris were initiated after the incident. The tests were performed by the U.S. Geological Survey (USGS) in Oregon, USA, with a 95 m long reinforced concrete channel of 2 m wide and 1.2 m deep (DeNatale et al, 1999). The experiments were conducted with barriers constructed of wire rope nets with different opening sizes (300 mm, 200 mm and 150 mm) and ring nets composed of 300 mm diameter steel rings. The nets were impacted by debris flows with volume of about 10 m^3 and flow velocities between 5 m/s and 9 m/s. The experiments demonstrated that the barriers were capable of mitigating such debris flows.

Other successful cases of using flexible barriers to arrest debris were reported by Roth et al (2004). In these cases, flexible rockfall barriers of energy rating ranging from 750 kJ to 1500 kJ retained hard inclusions of debris flows in natural streamcourses in Japan and Austria. The volumes of hard inclusions retained were 750 m^3 and 200 m^3 respectively.

Some flexible rockfall barriers have been modified by proprietary manufacturers with a view to mitigating debris flows and open hillslope landslides. Wendeler et al (2007) reported that flexible barriers equipped with additional intermediate cable ropes were installed in a natural drainage line in Illgraben, Switzerland. The width of the drainage line was up to 15 m. According to Wendeler et al (2007), these barriers can transfer up to 400 kN to the anchorage. Monitoring of the barrier commenced in 2005 and the barriers were subsequently hit by a series of debris flows in 2005 and 2006, with volumes ranging from 10,000 m^3 to 70,000 m^3 and velocity between 1.65 m/s and 4.8 m/s. The reported discharge rates of the debris flows ranged from 7.5 m^3/s to 24 m^3/s. Back calculations of the responses of the barrier were carried out using the numerical package FARO.

The performance of a flexible barrier in intercepting shallow open hillside landslides has been investigated by Bugnion & Wendeler (2010) using large-scale field tests in Veltheim, Switzerland. 50 m^3 saturated soil materials comprising gravels, sand and clay were released at the crest of a slope to simulate an open hillside landslide. The slope was 8 m wide, 41 m long with an average inclination of 30^o. Thickness and velocity of the soil materials were reported to be about 0.3 m to 0.5 m and 7 m/s to 11 m/s respectively. The flexible barrier was instrumented to measure tensile forces in the cable ropes. By assuming an impact load distribution acting on the cable ropes, the impact pressure on the barrier was estimated.

2.1 Overview of design methodology of debris-resistance flexible barrier

The design methodology for flexible barriers against debris flows based on the energy approach was proposed in early 2000 (Wartmann & Salzmann, 2002). The approach estimates the energy transferred from debris impacts to flexible barriers with an aim to assessing the debris-resisting capacity of the barriers. It was described in detail by Roth et al (2004) and Wendeler et al (2006). One of the key assumptions of the energy approach is that the barrier is only required to stop a certain amount of debris and that the arrested debris block would resist the remaining debris. According to Wartmann & Salzmann (2002), the effective mass, M (kg), of the debris to be arrested by the barrier is estimated as follows:

$$M = \rho \cdot Q_p \cdot T_{imp} \qquad \text{Eq. (1)}$$

where ρ (kg/m^3) is density of debris, Q_p (m^3/s) is peak discharge, and T_{imp} (s) is duration of impact to stop debris. Based on back analyses of selected flume tests and case histories, a maximum time of impact (T_{imp}) of 4 seconds was recommended by Wartmann & Salzmann (2002) and verified against several case histories by Roth et al (2004). The impact energy, E (in Joules), on the barrier was proposed to be taken as the kinetic energy of the debris with an effective mass M.

The field observations of debris flow events in Illgraben, Switzerland revealed that the energy approach could have limitations in modelling the debris impact process and hence the assessment of the debris-resisting capacity of flexible barriers. The limitations include the inability to estimate the effects of drag force that could be induced by debris overflow above a

barrier. Wendeler et al (2007) proposed a new methodology based on the force approach for designing flexible barriers against debris flows or open hillslope landslides. The force approach is elaborated in detail by Bartelt et al (2009). A multi-stage surge model is adopted in the approach. During the impact of each surge, cable forces can be estimated by assuming a dynamic impact pressure acting in combination with a hydrostatic loading. The dynamic impact pressure, p (kPa) is taken as follows:

$$p = \alpha \rho_d v^2 \qquad \text{Eq. (2)}$$

where α is dynamic pressure coefficient, ρ_d (Mg/m^3) is density of debris, v (m/s) is the debris velocity. The associated dynamic load would depend on, inter alia, material type, water content and velocity of debris. The value of α is an empirical coefficient established on the basis of back analyses of instrumented field tests. According to Bartelt et al (2009), the values of α is 2 for granular debris flow, and range from 0.7 to 1.0 for mudflow. Bugnion & Wendeler (2010) examined the instrumental data of the relevant field tests and reported that the value of α could be about 0.6 for open hillside landslide.

This force approach was applied in the design of flexible debris-resisting barriers in Milibach, Switzerland which successfully retained a certain amount of landslide debris, as reported by Wendeler et al (2012). Design of flexible barriers using the force approach has also been used in landslide and debris flow mitigation projects in different places such as Switzerland (Pederzani et al, 2009), Canada (Bichler et al, 2012), Scotland (Isofer, 2012) and New Zealand (Hind & McArdell, 2010).

2.2 Numerical tools for analyzing structural behaviour of flexible barriers

A flexible barrier system consists of steel posts fixed in position by uphill and/or lateral steel cable ropes. Suspending cables restrain the posts and span the netting. The netting may comprise a series of rings with a diameter of about 300 mm and made of 3 to 5 mm spiralled steel wires. Other forms of netting, for example, cable wires diagonally fixed with clamps, are also available in the market. Energy dissipation elements are installed onto the cable ropes to enhance the energy absorption capacity of the barrier system. The system is flexible with large deflection behaviour when subjected to dynamic impact load.

Load transfer amongst the structural components of the system and hence the load distribution could be complicated. Estimations of load in each component may not be straight forward and cannot be done through simple calculations. Therefore, suitable computer programs would be needed if a detailed structural analysis of the barrier system is required.

A computer program for structural analysis of flexible barriers has been developed by Nicot et al (2001) using an explicit numerical algorithm. Special attention has been paid to the modelling of the structural behaviour of ring nets. The program models ring net as a hexagonal mesh. The structural properties of the mesh were calibrated based on results of load tests on ring nets. The performance of the program was tested against a full-scale experiment of a falling rock block impacting on a flexible barrier.

Finite-element software package, FARO, originally developed by Volkwein (2004) to simulate rockfall barriers, was modified to simulate the behaviour of flexible barriers subject to pseudo-static areal loads resulting from impacts of debris flows or shallow landslides. FARO was developed to cater for simulation of ring net barriers. It adopts a spring model whereby the stiffness of a ring in the ring net is modeled by a pair of diagonal spring elements in a four-sided ring. It adopts a non-linear finite-element numerical procedure in determining stress and strain using the displacements. FARO has been calibrated against field test data of debris flows and open hillside landslides. Wendeler et al (2006) presented a comparison of the computed cable forces with that measured in the Illgraben debris flow tests.

Another program capable of analyzing flexible barriers is NIDA-MNN, which is developed by Chan et al (2012). The program was developed by modifying a non-linear finite-element structural package, NIDA, which has been used in numerous projects in Mainland China, Hong Kong and the UK. NIDA-MNN has been demonstrated to be capable of analysing large deformations of structural elements such as ring nets and energy dissipation devices. Elasto-plastic and large deflection features of these structural elements are considered and an efficient incremental-iterative procedure is adopted (Chan, 1988) for tracing force equilibrium within the barrier system. In a flexible barrier, netting is attached to cable ropes spanning across steel posts. The netting can slide along the cable ropes. Special 'sliding cable element' has been built into NIDA-MNN to simulate the sliding action of the netting. To realistically capture the behavior of the netting, frictional forces between

the contact points of the nets are considered in the calculations. This program has been verified against the published results of the Illgarben field test by Zhou et al (2011).

3. OPEN HILLSIDE FAILURE IN JORDAN VALLEY, HONG KONG

The open hillside landslide occurred on a west-facing terrain above a cut rock slope which was formed as part of a site formation project at the Jordan Valley in Hong Kong (Figure 1). Both the failed hillside and the man-made slope below are within the construction site. The flexible barrier has a total length of 128 m and was constructed as part of the site formation project. The height of the steel posts is 5 m. The role of the posts is to hold the netting in place for catching rockfalls. The netting was composed of ring nets. The opening of each ring is 350 mm. In order to capture small rock pieces or rock fragments, a secondary mesh with openings of about 60 mm was attached to the ring nets. The steel posts, each made of 140 mm × 140 mm steel hollow section with a steel thickness of 4 mm, are at 10 m spacing and supported on concrete pad footings of 400 mm × 400 mm in dimensions. The embedment depth of the footings is about 500 mm. The barrier has a design capacity of 1,000 kJ for retaining boulders with volume up to 1 m^3. Energy dissipation is designed to be achieved through the energy dissipation elements and deformable netting. A sketch showing a schematic design of the barrier system is shown in Figure 2.

The landslide was reported in December 2009. Interpretation of aerial photographs taken in November 2007 and July 2008 suggested that the failure should have occurred within this period. It was suspected that the landslide occurred during the heavy rainfall in June 2008. Prior to the site formation project, there is no past recorded landslide in the vicinity according to landslide database established by the GEO. Post-failure inspections revealed that the total volume of the landslide is approximately 110 m^3. The landslide source covers a plan area of 7 m (long) and 10 m (wide). The maximum depth of the landslide source was 3 m. Figure 3 shows a general view of the landslide site. The upper portion of the source area comprises predominately saprolitic terrain and is steeply inclined (>50°) with adversely oriented joints, whilst the lower portion comprises predominately matrix-supported debris overlying saprolite. The debris was dry at the time of inspection, and measured approximately 11 m long and 10 m wide. After the debris was removed, it could be seen that the lower portion of the landslide source area was sloping at 30° to 40°. Deposition of

debris extended approximately 12 m from the toe of rupture on a gently sloping (<10°) ground. It consisted of matrix-supported debris mixed with rounded to sub-rounded boulders and vegetation. Its thickness increased towards the frontal end of deposition. No sign of debris run-up against the netting was apparent.

The landslide debris struck one of the supporting posts, Post P1, near the southern end of the barrier and two netting panels adjacent to the post (i.e. netting panels spanning across Posts P2-P1 and Posts P1-P15). A plan showing the locations of the posts and the landslide affected area is presented in Figure 4. The debris was largely retained by the barrier and there were no signs of overflow or marks left behind by a large amount of debris passing through the netting. However, Post P1 was severely damaged by debris impact (Figure 5). Post P15, located at the southern end of the barrier, had also been bent, although it was not subject to any direct impact by the landslide debris (Figure 6). Both Posts P1 and P15, together with their concrete footings, were found to have displaced forward by about 1 to 2 m. No signs of damage to Post P2 were evident (Figure 7). It is noteworthy that the construction details of Post P15 are different from the intermediate Posts P1 and P2. The netting was attached to Post P15 by about nine layers of stainless steel bands (Figure 8), whereas Posts P1 and P2 were not tied to any net. These details might have contributed to the failure of Post P15 despite that it was not impacted by landslide debris directly. The failure of the post may also be linked to rigid connection between the post and the foundation, which is the weakest point of the barrier. If the connection between the post-plate and the foundation was able to dissipate some of the impact energy, failure of the post may not have occurred. It was also observed during the inspections that the energy dissipation devices attached to the uphill cable ropes of the barrier had not been mobilised, and no tensile failure of any cable ropes was apparent. Energy dissipating elements which are able to dissipate the energy by the deformation of their elements are preferred to the one that works with friction (i.e. friction of the cables).

4. DEBRIS MOBILITY ASSESSMENT OF THE LANDSLIDE

A mobility assessment of landslide debris is carried out using computer program 2d-DMM developed by Kwan & Sun (2006). Figure 9 shows a cross-section along the centerline of the landslide debris trail. The travel angle of the landslide debris, given the

retarding effect of the flexible barrier, is about 27^o. This travel angle does not represent the true mobility of the landslide debris because the debris was obstructed by the flexible barrier. If frictional rheology is adopted to back analyse the landslide mobility, an apparent basal friction angle (ϕ) of less than 27^o should be used. GEO (2012) presents a review of the mobility of open hillside landslides in Hong Kong. The review shows that the lower bound value of ϕ for open hillside landslides in Hong Kong is 25^o for landslide volume less than 500 m^3. The ϕ value of this Jordan Valley landslide therefore could be in the range of 25^o to 26^o, and a ϕ-value of 25^o has been adopted in the mobility analysis.

Landslide debris is modelled as a homogeneous continuum material in the analysis of 2d-DMM. An explicit Lagrangian numerical scheme proposed by Hungr (1995) to solve the governing equations of unsteady non-uniform shallow water flow equations is adopted. The computational grid divides the landslide into a number of mass blocks. The formulation calculates the velocity of the computational grid. The computer program had been calibrated against over 70 open hillside landslide cases in Hong Kong (GEO, 2012).

The geometry of the runout path and the initial debris profile at the landslide source determined based on the field mapping and the cross-section shown in Figure 9 have been adopted for the debris mobility analysis. The debris velocity and debris thickness hydrographs at the location of the barriers have been obtained from the analysis. Figures 10 and 11 present the hydrographs. The analysis shows that debris could have reached the barrier at about 4 seconds after the landslide. The maximum frontal debris velocity at the location of the flexible barrier could be around 4 m/s. After the peak value, the velocity drops to zero within 2 seconds. The calculated debris thickness is within the range of 0.8 m to 1.2 m, which is generally consistent with the site observations that the debris deposit was about 1 m thick. Since the debris velocity could have dropped rapidly and the debris could be as thick as about 1 m, it is considered unlikely that the rear portion of debris mass over-rode on the frontal portion to result in multiple impacts to the barrier.

5. STRUCTURAL ANALYSIS OF THE FLEXIBLE BARRIER

Computer program NIDA-MNN has been used for the structural analysis. The two netting panels of the rockfall barrier spanning across Posts P1, P2 and P15, which were struck

by landslide debris, are considered in the numerical analysis. The structural model of the flexible barrier, which is an assembly of netting, steel posts, rope cables, etc. has been set up based on the detailing and the physical dimensions of different structural components shown on the as-built drawings of the barrier. No energy dissipation device is considered in the analysis, since the site inspection revealed that the energy dissipation devices were not mobilised.

The barrier is a proprietary product. Contacts with the manufacturer of the barrier had also been made to confirm the structural properties of different components of the barrier (e.g. ultimate yield strength of cable ropes, etc.) to facilitate the structural assessment. Details such as dimensions of the structural components are given in Annex A. The post foundations are modelled as pin supports, since the shallow footing could not have provided a high rotational restraint. This agrees with the site observation that the footings of Posts P1 and P15 significantly rotated following the impact of the landslide debris. Sliding of the footing is not considered by the structural analysis, which allows calculation of the induced base reaction prior to movement of the foundation. The model set-up and the assumed boundary conditions are shown in Figure 12.

The debris impact load is modelled as a pseudo-static uniformly distributed pressure (UDP) acting orthogonally on the barrier. Site observation suggests that landslide debris could have impacted on Post P1 and the netting on the two sides of the post. Based on the results of the debris mobility analysis as well as site observations, it is estimated that the thickness of debris hitting the barrier could be of the order of 1 m. In light of this, the loaded area of UDP against the netting and Post P1 is assumed to be 1 m high. A uniform thickness is assumed in the analysis. The width of the UDP is taken as 10 m, which is the observed width of the landslide. The loaded area of UDP is centered at Post P1 to tally with the site inspection (see also Figure 12). A single impact is considered in the back analysis, since no evidence of multiple surge impacts was identified on site. The magnitude of the uniformly distributed pressure (UDP) applied to the barrier increased until failure of any post or cable rope occurs.

NIDA-MNN analysis indicates that the steel posts could have been subjected to an axial load together with bending moments about both of the principal axes of the cross section.

Failure of the posts can be checked using the plastic analysis recommended in the Code of Practice for Structural Uses of Steel, Hong Kong (BD, 2011). According to BD (2011), buckling failure of a column would take place when the section capacity factor (*R*) as defined in Eq. (3) is greater than unity.

$$R = \frac{P}{P_{sq}} + \frac{M_x}{M_{CX}} + \frac{M_y}{M_{CY}} \qquad \text{Eq. (3)}$$

where

P = calculated axial force

M_X, M_Y = calculated bending moments about x- and y- axes

M_{CX}, M_{CY} = bending moment capacity about x- and y- axes

P_{sq} = squash load = σ_{yield} × sectional area

σ_{yield} = critical yield strength (174 MPa in this case history)

Shear failure of the posts has been checked using Eq. (4) below:

Shear failure is not permissible if $V / V_c < 1$ Eq. (4)

where V = calculated shear stress

V_c = allowable shear stress

Based on the site inspections, Posts P1 and P15 failed but not P2. Different magnitudes of UDP are used in the analysis with a view to replicating the observations numerically. Results show that both Posts P1 and P15 could fail by buckling when the applied UDP was increased to 50 kPa. The large bending moment in P1 is induced by the UDP directly acting on the post, whereas the bending moment in P15 is induced by the lateral deformation of the netting attached to it. Failure of both P1 and P15 is due to the combined actions of bending moment and axial compression load. The combined actions could have resulted in buckling failure of the posts. For P15, analysis shows that the post could have been subjected to bending moments and shear forces induced by load transferred from the netting attached to the post. In addition, P15 could have experienced an axial compression load larger than that in P1. This larger compression load could be due to the downward forces brought about by both the uphill and the lateral anchor cables attached to the top of the post, as well as the

deformed netting that was connected to the post. This may explain the reason for the failure of P15, which was not subject to a direct hit by the landslide debris. The shear forces induced in the posts were found to be not critical in terms of the structural capacity. The analysis also shows that the calculated maximum deformation of the netting is about 2.5 m. The order of magnitude of the calculated deformation generally agrees with the site measurement. The calculation results for P1, P2 and P15 are summarised in Table 1.

An attempt to estimate the upper limit of the applied UDP to cause an overall failure of the barrier has been made. It is noted that when the applied UDP is increased to 66 kPa, the calculated tension developed in the lower cable ropes reaches the ultimate tensile strength of 270 kN. Therefore, analysis based on UDP of magnitude exceeding 66 kPa has not been undertaken. The computed deformations of the flexible barrier panels and the calculated bending moment and shear force diagrams on the posts for an UDP of 66 kPa respectively are shown in Figures 14 to 15. In all the analyses, the calculated forces in Post P2 remained low. Structural assessments indicate that these calculated forces do not exceed the structural capacity of Post P2, which is consistent with the site observation that Post P2 was undamaged.

To investigate the critical load transfer between netting and post, an additional numerical analysis which does not consider the attachment of the netting to Post P15 is carried out. Results of the additional analysis show that while there is no significant change in bending moment (M_x) of Post 1, bending moment (M_y) experienced by Post P15 could be significantly reduced by 95% at UDP of 66 kPa, and no buckling failure of Post 15 could have been resulted in. It is concluded that the effect of load transfer from the netting attached on the post could be critical and should be carefully considered in the design.

The calculated base horizontal reaction in *y*-direction of Post P1 is in the order of 350 kN to 450 kN for the range of UDP (i.e. 50 kPa to 66 kPa) considered in this study. It is very likely that this reaction force has exceeded the sliding resistance of the shallow footings of the posts. As such, the corresponding footings displaced from their original locations as observed but this was not modeled in the analysis. Toe failure of P15 is also observed on site and this is probably due to lateral deformation of the netting attached to the post.

However, the post-failure mechanism is not modelled by the present analysis, since a pin connection at the base of the posts is assumed.

It is acknowledged that the present back analyses only provided an approximate indication of the possible load transfer pattern of the flexible barrier through sensitivity analysis. The analyses are subject to the following limitations: (i) the simulations do not consider the post-failure mechanisms of the structural system and the post foundations, such as redistribution of loads among the structural elements of the barrier system and the possibility of progressive failure, and (ii) the weight of debris retained in the bulged portion of the netting is neglected. The results of the present analyses suggest the possibility of both foundation failure and buckling failure of the two posts, however, the actual sequence of failure cannot be determined. In spite of these limitations, the back analyses provided a basis for sensitivity analyses to gauge the possible load transfer mechanism of a flexible barrier upon debris impact.

6. DISCUSSION

6.1 Force and Energy Considerations

In current practice, some designers would adopt Eq. (2) to calculate the dynamic pressure of debris impacting on a flexible barrier. The UDP applied in the above structural analysis simulates the dynamic impact pressure of landslide debris hitting the flexible barrier. Having worked out the range of the UDP which lead to computed behaviours that replicates the site observations, the dynamic pressure coefficient (α) can be back calculated for the Jordan Valley landslide case. The above structural assessments indicate that the effective UDP could be in the range of 50 kPa to 66 kPa. If the debris density is assumed to be 2,000 kg/m^3 and debris impact velocity is taken to be 4 m/s based on the debris mobility analysis, the value of α would be in the range of 1.6 to 2.1.

Investigation of this case history can also be undertaken from the energy perspective. The theoretical kinetic energy (KE) of landslide debris that travelled beyond the original barrier location can be estimated by coupling together the debris velocity hydrograph (Figure 10) and debris thickness hydrograph (Figure 11) using the following equation:

$$KE = \sum_{t} \frac{1}{2} [v(t)\ h(t)\ w\ \rho\ \Delta t][v(t)]^2 \qquad \text{Eq. (5)}$$

where $v(t)$ = debris velocity at barrier location at time t (m/s)

$h(t)$ = debris thickness at barrier location at time t (m)

w = debris width at barrier location, assumed to be constant

ρ = debris density (in kg/m^3)

Δt = observation time interval (s)

According to the site inspection, debris width (w) is about 10 m. Debris density is assumed to be 2,000 kg/m^3. With the velocity and debris hydrographs computed by the debris mobility analysis, the kinetic energy of the debris is estimated to be 463 kJ using Eq. (5). The calculation of kinetic energy using the equation does not consider the obstruction effect due to the barrier and it corresponds to the KE at an "uninterrupted" state. In theory, this is the upper bound energy loading that could be applied on the barrier.

NIDA-MNN computes strains in the structural elements of the barrier system. Based on the computed strains, the strain energy in the barrier system as a result of landslide impact can be obtained. The strain energy is 60 kJ when the UDP is 50 kPa. The difference in this strain energy and the upper bound energy loading may be attributed to energy dissipation due to failure of the post foundations and plastic deformation of the posts, both of which are not considered in the analysis. Annex B presents simplified estimates of these two energy dissipations. It is shown that energy dissipations due to failure of the post foundations and plastic deformation of the posts could be 176 kJ and 44 kJ respectively. The sum of the strain energy and these two energy dissipations is 280 kJ. This value presents an approximate order of magnitude of the energy dissipation involved in the landslide impact. It corresponds to 61% of the upper bound energy loading. A higher figure could be obtained if frictional loss within the flexible barrier system (e.g. energy loss due to friction between rings in netting) is taken into account. However, an accurate estimation of the frictional loss is not possible.

6.2 Design considerations for the robustness of barriers

Based on the field observations and the analyses above, some design considerations that are critical to the robustness of flexible debris-resisting barriers are identified and summarised as follows:

(a) the combined action of axial force and bending moment induced by debris impact and the downward force of uphill cable ropes and lateral cable ropes could be critical to the post design and should be checked,

(b) the location of debris impact load on barrier should be carefully chosen for design checks, as in some cases loading acting on the end panel of the barrier could constitute one of the critical loading cases for the design of end posts,

(c) detailing, especially connections of structural elements (e.g. attachment of netting to posts and connection of post and base plate) should be duly considered and the use of ductile connection between post and base plate could provide a practical means in achieving additional energy dissipation,

(d) the need for checking the structural performance of barrier posts and energy dissipating elements that are not directly hit by landslide debris should not be overlooked,

(e) the foundations of barrier posts should be properly designed and reinforced to guard against possible sliding failure due to debris impact on the barrier, and

(f) due attention should be paid to proper detailing in order to ensure the effective mobilisation of the energy dissipating elements as per the design intent.

Site inspections revealed that the energy dissipating elements attached to the uphill anchor cables were not activated and hence item (f) above is suggested. Based on the details shown on the as-built records, the cables were threaded through small holes (120 mm in diameter) in the barrier posts and were connected to the top and bottom ropes. Activation of

the energy dissipating elements would have required adequate extension of the uphill cables before failure of the posts. According to the design package of the rockfall barrier, the uphill cables are supposed to slide through the holes in the posts, in order to create sufficient cable extensions so as to mobilise the energy dissipating elements (Figure 16). However, it was observed that there was little movement of the cables relative to the posts (Figure 17). The friction between the cable and the post could have restrained the movement of the cable and this might be one of the factors that led to the observed non-performance of the energy dissipating elements. Displacement and deformation of the posts resulting in structural failure and foundation failure could also have played a role in this regard, as these could have affected the movement of the cable through the hole in the post. Apart from the above, there could be other possible contributory factors. The energy dissipating elements of the flexible barrier were positioned close to the ground surface and as such, they might have been buried by landslide debris when the barrier was struck, which could impede the mobilisation of the brake elements.

It would be beneficial in terms of design robustness if the post foundation be able to dissipate energy during the impact. However, the energy dissipation would be associated with a certain amount of deformations or movements, which calls for repairing works afterwards. The repairing work for foundation is difficult and the performance of foundation involving deformations or movements is not easy to ascertain.

There have been reported case histories that flexible rockfall barriers intercepted snow avalanches in Europe. Although flexible rockfall barriers could stop certain type of snow avalanches, barriers were found damaged by snow avalanches of high energy level. Impact load patterns induced by snow avalanches and landslide debris could be similar. They could be both represented by areal loads. Some of the observations made by Margreth & Roth (2008), who examined some of the flexible rockfall barriers damaged by snow avalanches in Austria, are consistent with the present study. Margreth & Roth (op cit) summarised their observations made over four winters from 2003 to 2006. They noted that barrier post foundations could be vulnerable to damage when barriers are subject to impact by snow avalanche, and recommended that post foundation should be properly reinforced and post spacing be reduced. It should be emphasised that flexible rockfall barriers could only retain

certain amount of landslide debris/snow avalanche. They may not be capable of stopping high energy level events.

In the present case study, the foundations of two of the barrier posts failed upon the impact of landslide debris. The rigid connection at the post and the base plate could have played a role in this respect. Numerical analyses indicate that the loading on the post foundations in the Jordan Valley barrier could have been up to about 350 kN to 450 kN which was liable to cause sliding failure. Attention to the loading on post foundation of barriers subjected to landslide debris impact is warranted in future research.

7. CONCLUSIONS

A case study of an open hillside landslide impacting on a flexible rockfall barrier has been investigated and back analysed. The study comprised field inspections, debris mobility assessment and structural analyses. It is noted that although the landslide debris was largely arrested by the flexible barrier, two barrier posts were severely damaged. The debris mobility assessment and structural analyses have managed to reproduce the key salient field observations. Sliding failure of the post foundation and buckling failure of the posts are inferred by the structural analysis. The key contributing factors to the post failure were highlighted. Connection details of the netting and post are considered crucial in governing the load transfer between the two components. The importance of detailing that facilitates the mobilisation of energy dissipating elements is also emphasised by this case study.

Given that there are no instrumented data (e.g. measured cable forces, etc.) for calibration purposes, the back calculated parameters (e.g. the dynamic pressure coefficient) cannot be properly verified. However, the sensitivity analyses provided an estimate of the possible behaviour of the flexible barrier upon debris impact, and the deduced values of α being in the range of 1.6 to 2.1 do not appear unreasonable. The pseudo-static approach adopted in the structural analysis of this study has some limitations. Further study should include numerical analyses which combine debris mobility modelling and structural assessment, and large-scale instrumented tests of flexible barriers subject to debris impact.

8. ACKNOWLEDGMENTS

This paper is published with the permission of the Head of Geotechnical Engineering Office and the Director of Civil Engineering and Development of the Government of the Hong Kong Special Administrative Region.

9. REFERENCES

BD (2011). Code of Practice for the Structural Use of Steel 2011, Buildings Department, HKSAR Government, Hong Kong.

Bartelt, P, Volkwein, A., & Wendeler, C. (2009). Full scale testing and dimensioning of flexible debris flow barriers. Summary report of the 2005-2008 CTI-Project "Numerical modeling and design of flexible debris flow barriers". Swiss Federal Institute for Forest, Snow, and Landscape Research (WSL), Switzerland.

Bichler, A., Yonin, D., & Stelzer, G. (2012). Flexible debris flow mitigation: Introducing the 5.5 Mile debris fence. Landslides and Engineered Slopes Protecting Society through Improved Understanding, *Edited by* E. Eberhardt, C. Froese, A.K. Turner and S. Leroueil, CRC Press, pp. 1955-1960.

Bugnion, L. & Wendeler, C. (2010). Shallow landslide full-scale experiments in combination with testing of a flexible barrier. Monitoring, Simulation, Prevention and Remediation of Dense and Debris Flows III. *Edited by* D. De Wrachien & C.A. Brebbia, WIT Press, pp. 161 - 173.

Chan, S.L. (1988). Geometric and Material Nonlinear Analysis of Beam-Columns and Frames using the Minimum Residual Displacement Method, International Journal for Numerical Methods in Engineering, **26**: 2657-2669.

Chan, S.L., Zhou, Z.H. & Liu, Y.P. (2012). Numerical analysis and design of flexible barriers allowing for sliding nodes and large deflection effects. *In* Proceedings of the One Day Seminar on Natural Terrain Hazards Mitigation Measures, 16 October 2012,

Hong Kong. *Edited by* C.K. Lau, Eddie Chan and Julian Kwan, The Association of Geotechnical and Geoenvironmental Specialists (Hong Kong) Limited, pp. 29-43.

DeNatale, J.S., Iverson, R.M., Major, J.J., LaHusen, R.G., Fiegel, G.L. & Duffy, J.D. (1999). Experimental Testing of Flexible Barriers for Containment of Debris Flows. USGS Open-File Report 99-205, US Geological Survey.

Duffy, J.D. (1998). Case studies on debris and mudslide barriers systems in California. *In* Proceedings of the One Day Seminar on Planning, Design and Implementation of Debris Flow and Rockfall Hazards Mitigation Measures, Hong Kong, 27 October 1998. *Edited by* C.K. Lau, R.P. Martin and K.T. Chau, The Association of Geotechnical Specialists (Hong Kong) Ltd. and The Hong Kong Institute of Engineers (Geotechnical Division), pp. 77-90.

GEO (2012). Guidelines on Assessment of Debris Mobility for Open Hillslope Failures, (Technical Guidance Note No. 34). Geotechnical Engineering Office, HKSAR Government.

Hind, K.J. & McArdell, B.W. (2010). Numerical modelling of debris-flows and mitigation structures at Matata, New Zealand. *In* Geologically Active: Proceedings of the 11th IAEG Congress. Auckland, New Zealand, 5-10 September 2010. *Edited by* A.L. Williams, G.M. Pinches, C.Y. Chin, T.J. McMorran and C.I. Massey, CRC Press, pp. 3003-3010.

Hungr, O. (1995). A model for the runout analysis of rapid flow slides, debris flows and avalanches. Canadian Geotechnical Journal, **32**: 610-623.

Isofer (2012). TranServ - Trunk Road Network North West Scotland A83 Rest and be Thankful - Phases 3 and 4 Debris Flow and Shallow Landslide Protection. Isofer AG, Switzerland.

Kwan, J.S.H. & Sun, H.W. (2006). An improved landslide mobility model. Canadian Geotechnical Journal, **43**: 531-539.

Margreth, S. & Roth, A. (2008). Interaction of flexible rockfall barriers with avalanches and snow pressure. Cold Regions Science and Technology, **51**: 168-177.

Nicot, F., Cambou, B., & Mazzoleni, G. (2001). From a constitutive modeling of metallic rings to the design of rockfall resisting nets. International Journal for Numerical and Analytical Methods in Geomechanics, **25**: 49-70.

Pederzani, A., Calegari, L., Guasti, G., Balatti, F. & Fasola, R. (2009). Flexible Ring Net Barriers Preferred to Concrete Works: the Riale Buffaga Experience (Ronco s./Ascona, Switzerland), Technical Documentation, February 2009, Geobrugg AG, Switzerland.

Roth, A., Kästli, A. & Frenez, Th. (2004). Debris flow mitigation by means of flexible barriers. Proceedings of the International Symposium Interpraevent 2004, Trento, Italy.

Volkwein, A. (2004). Numerical Simulation of Flexible Rockfall Protection Systems. PhD Thesis, Swiss Federal Institute of Technology Zürich, Switzerland *(In German)*.

Wartmann, S. & Salzmann, H. (2002). Debris flow and floating tree impacts on flexible barriers. *In* Proceedings of the Conference on Natural Terrain - A Constraint to Development, Hong Kong, 14 November 2002. Institution of Mining and Metallurgy, Hong Kong Branch, pp. 125-131.

Wendeler, C., McArdell, B.W., Rickenmann, D., Volkwein, A., Roth, A. & Denk, M. (2006). Field testing and numerical modelling of flexible debris flow barriers. *In* Proceedings of the Sixth International Conference of Physical Modelling in Geotechnics, Hong Kong, 4-6 August 2006. *Edited by* C.W.W. Ng, L.M. Zhang, and Y.H. Wang, pp. 1573-1604.

Wendeler, C., Volkwein, A., Denk, M., Roth, A. & Wartmann, S. (2007). Field measurements used for numerical modelling of flexible debris flow barriers. *In* Proceedings of Fourth International Conference on Debris Flow Hazards Mitigation: Mechanics, Prediction, and Assessment, Chengdu, China, 10-13 September 2007.

Edited by C.L. Chen and J.J. Major, pp. 681-687.

Wendeler, C., Haller, B. & Salzmann, H. (2012). Protection against debris flows with 13 flexible barriers in the Milibach River (Canton Berne, Switzerland) and first event Analysis. *In* Proceedings of the One Day Seminar on Natural Terrain Hazards Mitigation Measures, 16 October 2012, Hong Kong. *Edited by* C.K. Lau, Eddie Chan and Julian Kwan, The Association of Geotechnical and Geoenvironmental Specialists (Hong Kong) Limited, pp. 22-28.

Zhou, Z.H., Liu, Y.P. & Chan, S.L. (2011). Nonlinear finite element analysis and design of flexible barrier (Project Report). The Hong Kong Polytechnic University.

FIGURES

Figure 1 An overall view of the landslide site

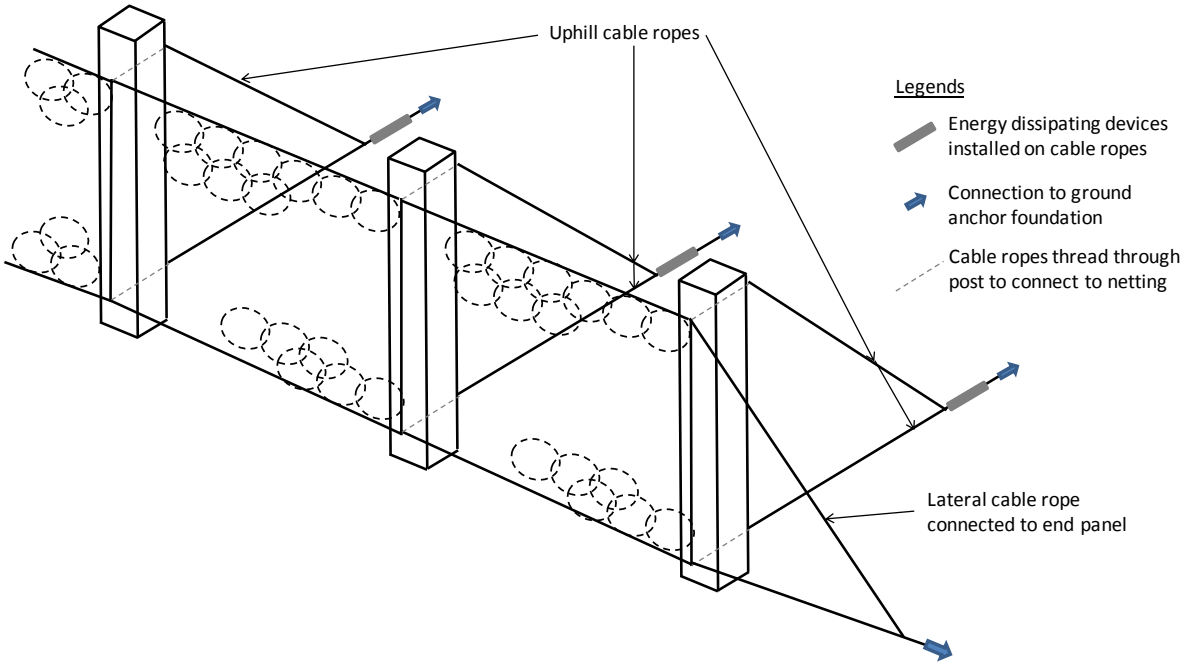

Figure 2 Set-up of the flexible rockfall barrier

Figure 3 The landslide scar and the flexible rockfall barrier

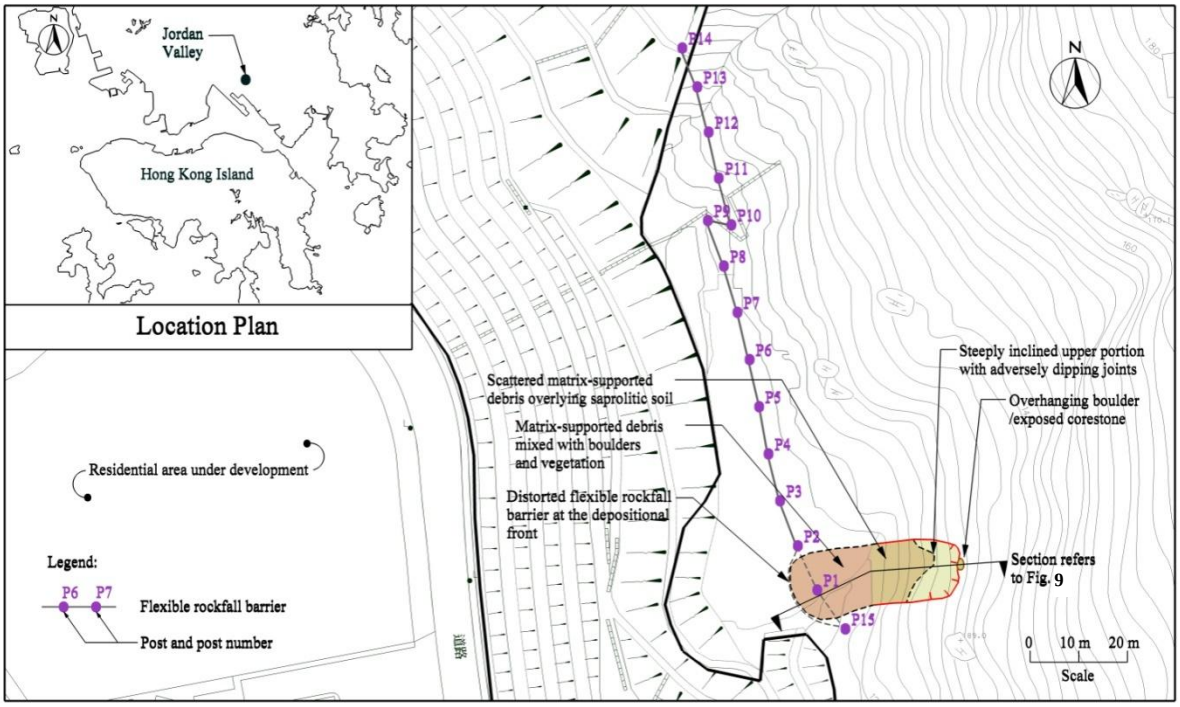

Figure 4 Locations of the landslide and the posts of the flexible barrier

Figure 5 Post P1 damaged; landslide debris was largely contained by the barrier

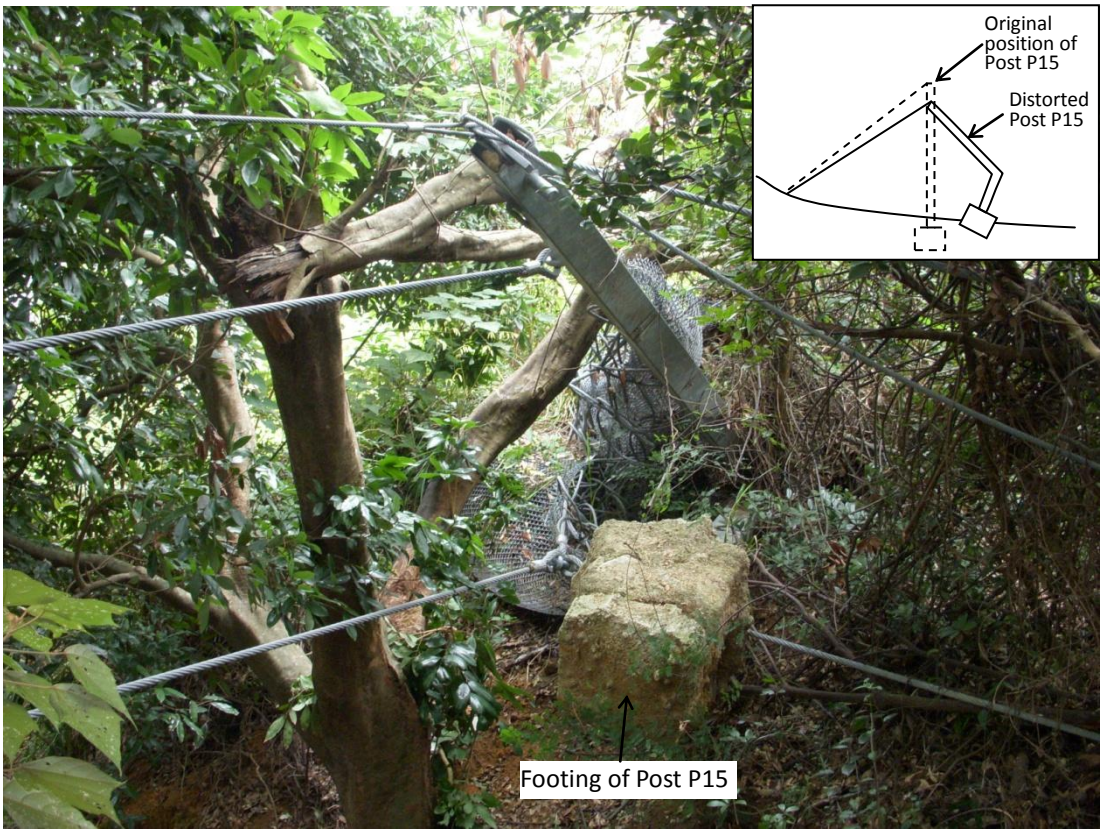

Figure 6 Post P15 severely bent and foundation failed

Figure 7　Post 2 undamaged

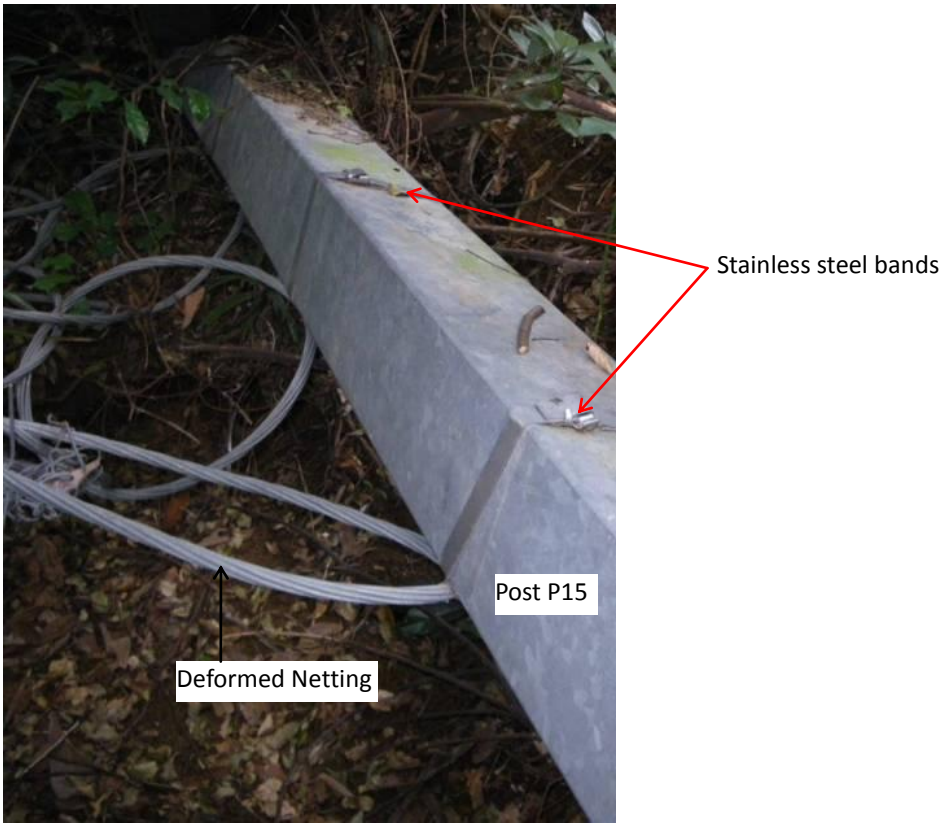

Figure 8　Netting attached to Post P15 using stainless steel bands

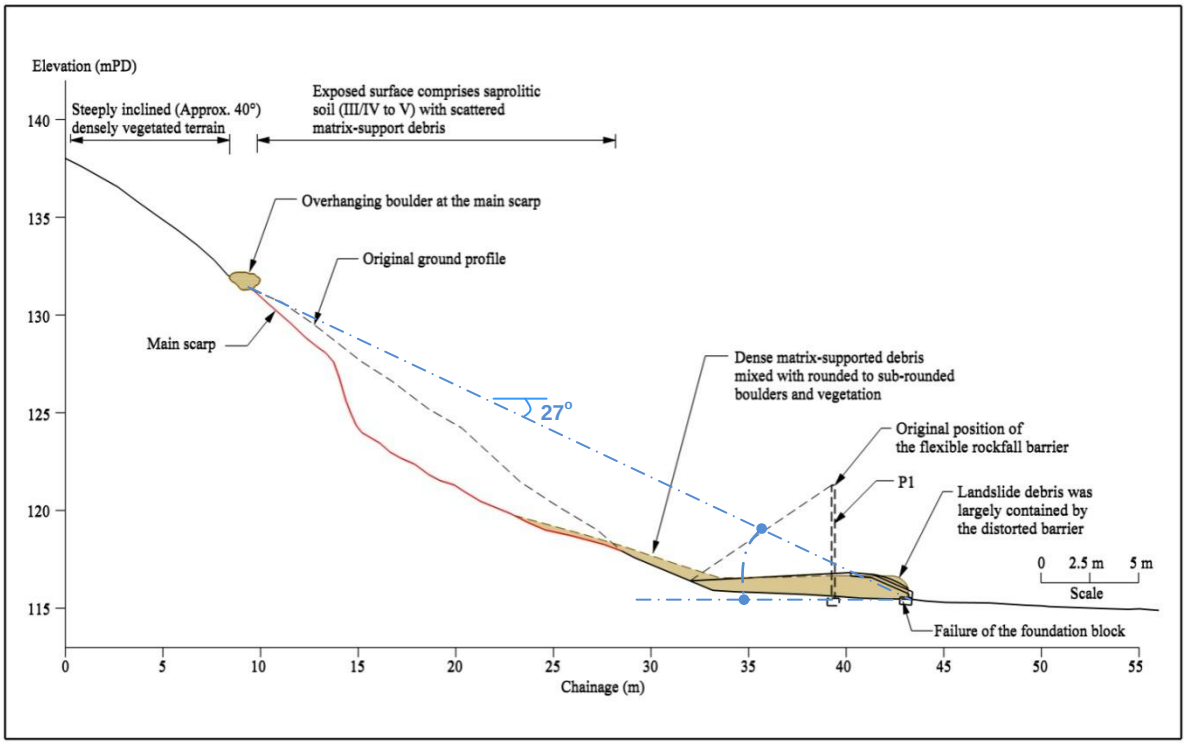

Figure 9 Cross-section along the centreline of the landslide

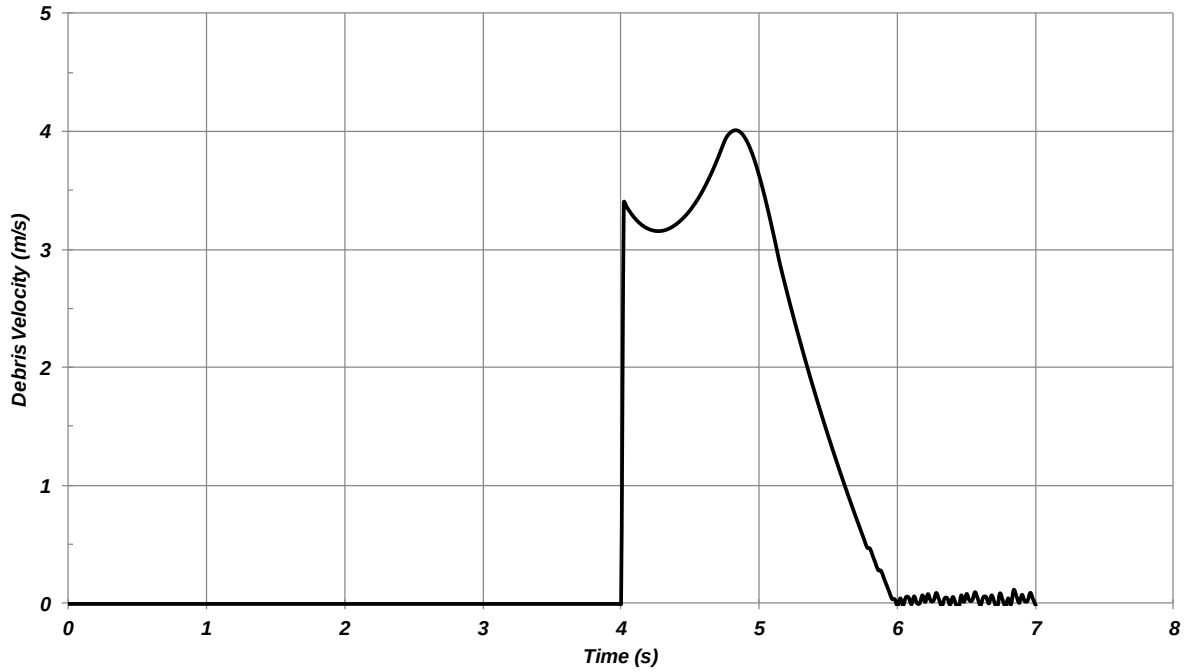

Figure 10 Debris velocity hydrograph at the barrier location

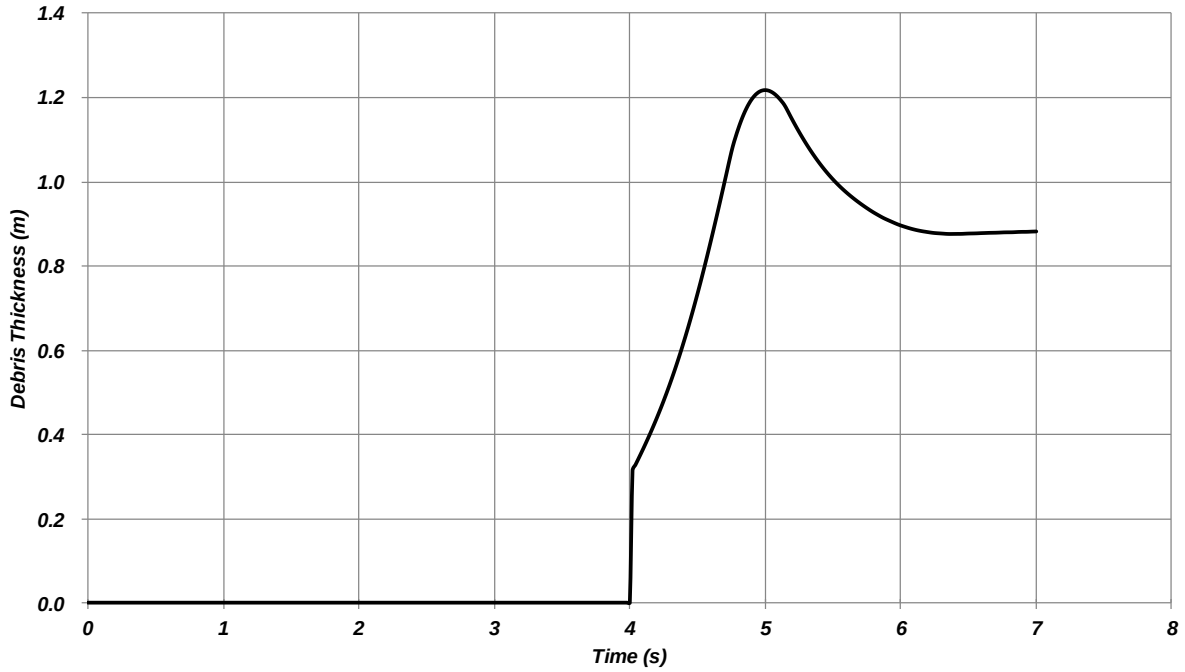

Figure 11 Debris thickness hydrograph at the barrier location

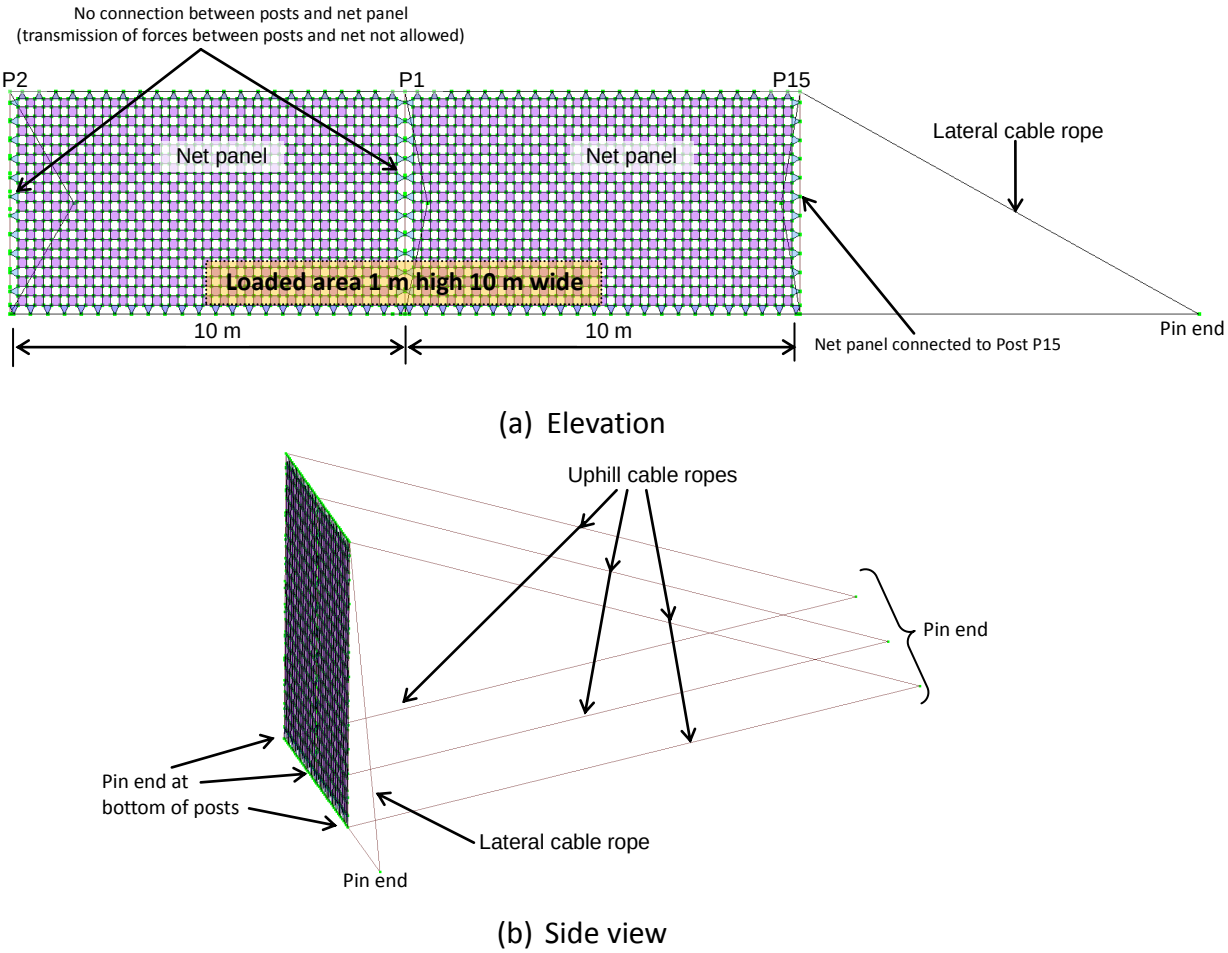

Figure 12 Model set up for the structural analysis

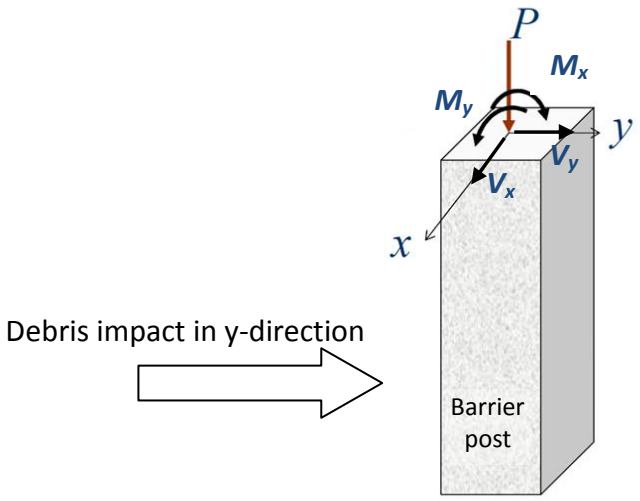

Figure 13 Symbols of Eq. (3)

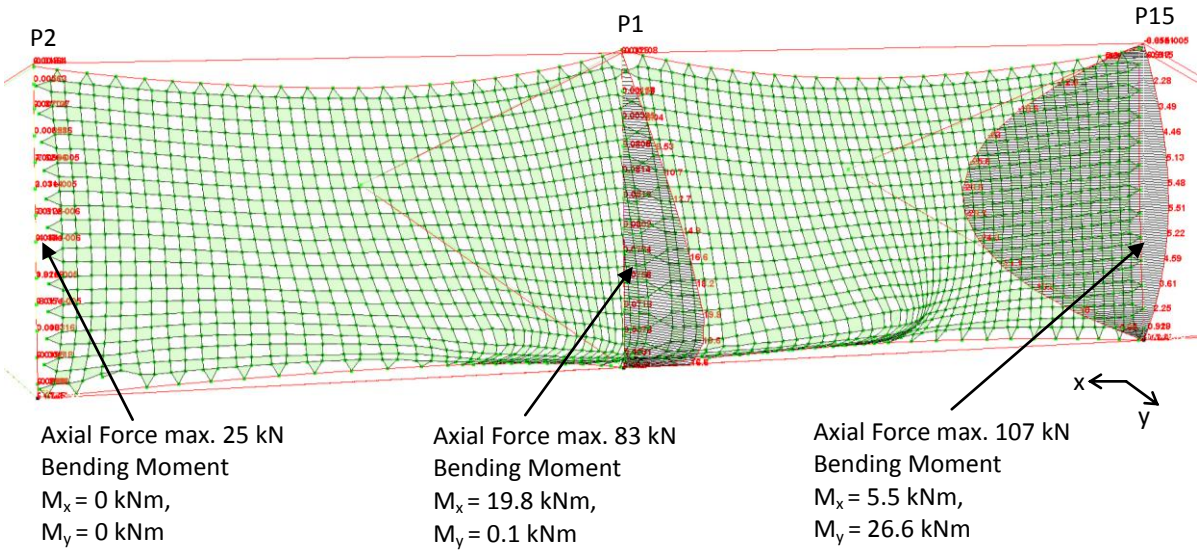

Figure 14 Bending Moment Diagrams of the Posts under UDP of 66 kPa

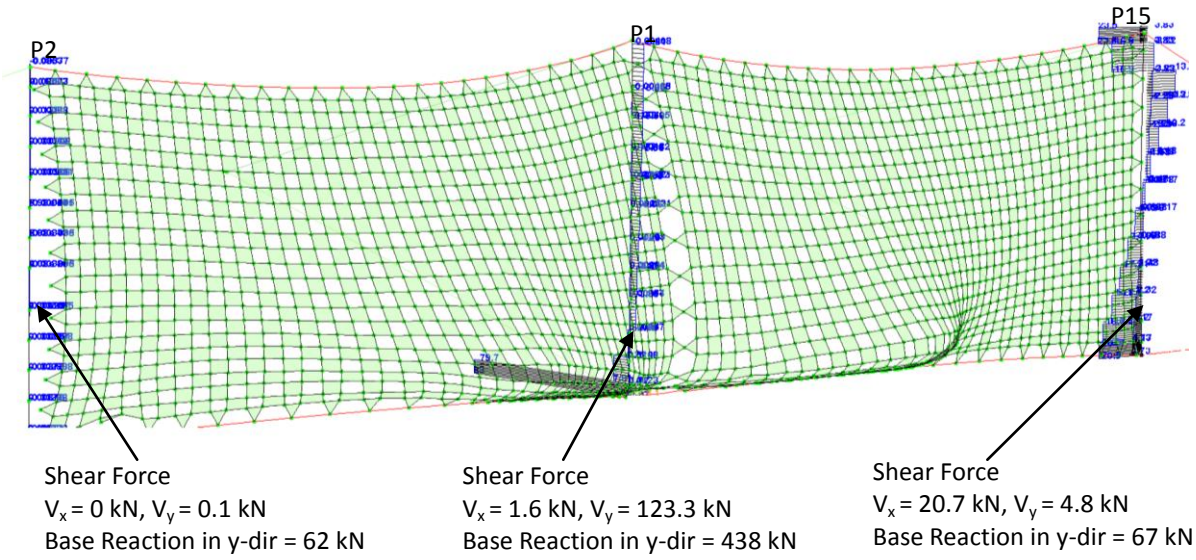

Figure 15 Shear Force Diagrams of the Posts under UDP of 66 kPa

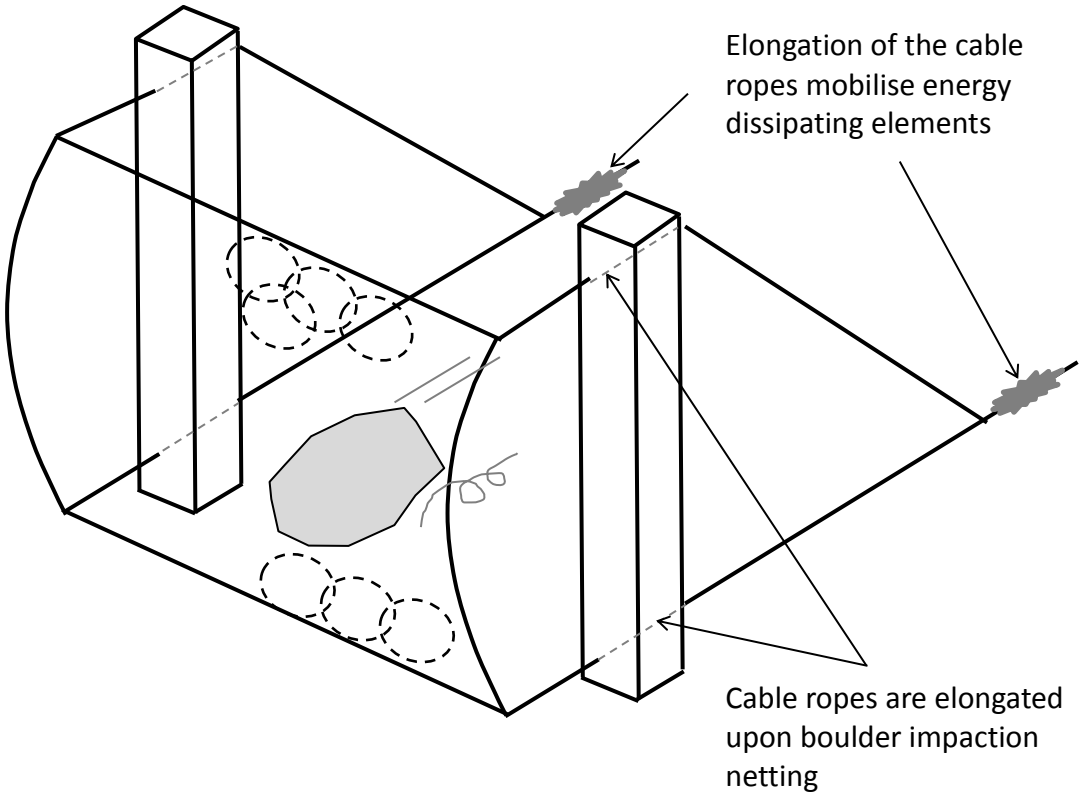

Figure 16 Mobilisation mechanism of energy dissipating element

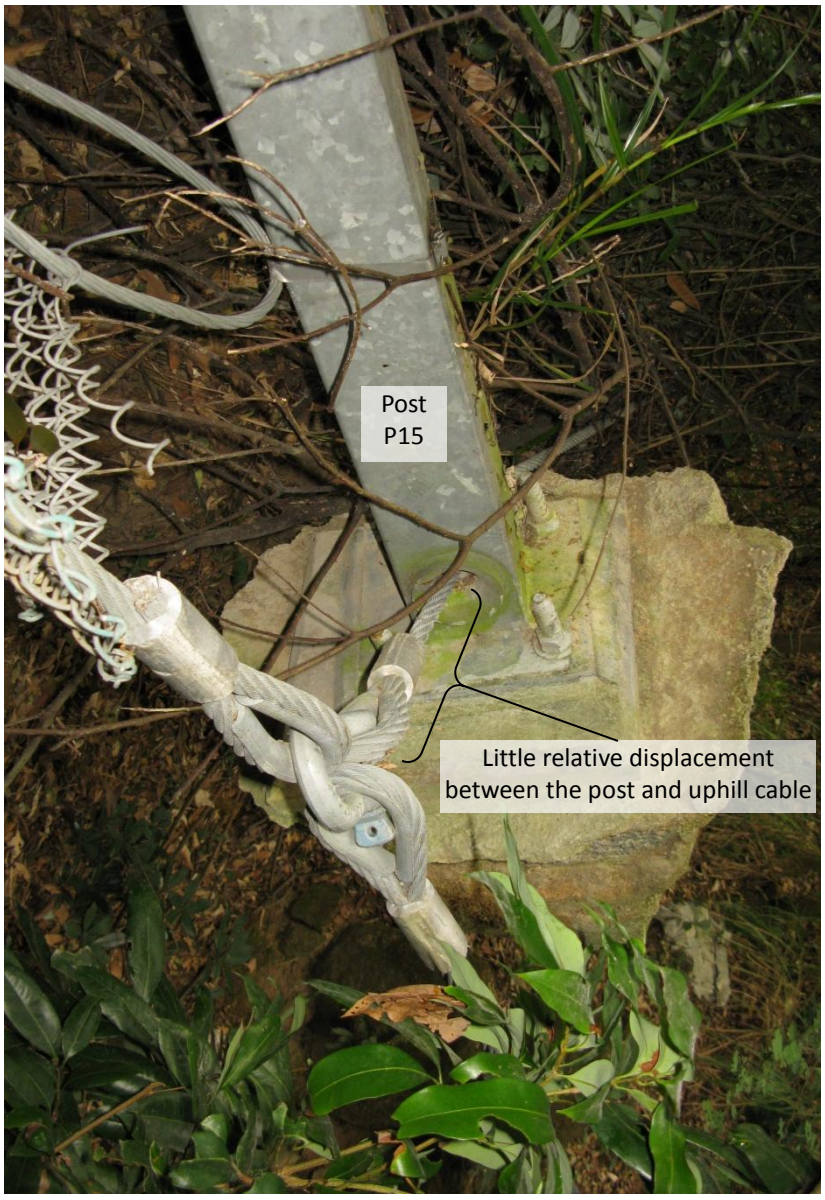

Figure 17 Little relative displacement between barrier post and uphill cable observed

Table 1 Results of the structural analysis

UDP (kPa)	Post No.	Calculated maximum axial compressions and bending moments in posts			Section Capacity factor (R) (Eq. (3))	Other calculated maximum forces			
		P (kN)	M_x (kNm)	M_y (kNm)		V_x (kN)	V_y (kN)	Post base horizontal reaction in y-dir. (kN)	Cable force (kN)
50	P2	21	0	0	0.1	0	0	47	227
	P1	68	13.9	0.2	1.0*	1.2	86.6	333	227
	P15	92	4	20.4	1.6*	15.6	3.4	51	227
66	P2	25	0	0	0.1	0	0.1	62	271^
	P1	83	19.8	0.1	1.4*	1.6	123.3	438	271^
	P15	107	5.5	26.6	2.1*	20.7	4.8	67	271^

*Post fails in buckling
^Cable fails in tension

Annex A - Properties and Dimensions of the Structural Components of the Barrier adopted in Setting Up the Structural Model

Ring net

1) Diameter of ring: 350 mm
2) Diameter of ring wire: 3 mm (7 spirals)
3) Six rings connection

Hollow steel post

1) Height: 5 m
2) Size: 140 mm x 140 mm
3) Thickness: 4 mm
4) Radius of gyration: 55.2 mm
5) Cross section area = 2.14×10^3 mm^2
6) Moment of inertia = 6.52×10^6 mm^4
7) Section modulus = 93.1×10^3 mm^3
8) Yield stress = 235 MPa
9) Elastic modulus = 200 GPa
10) Founded on shallow concrete footing of dimensions 400 mm x 400 mm x 500 mm depth

Energy dissipating device

The energy dissipating devices attached to the uphill cables were not activated as observed during the site inspections. Energy dissipating device is therefore not included in the structural model.

Extension rope cables

1) Diameter of top rope cable is 20 mm (6 threads of 19 wires)
2) Diameter of bottom rope cable is 20 mm (6 threads of 19 wires)
3) Tensile failure load is 270 kN

Annex B - Estimation of energy dissipation by plastic deformations of barrier posts and failure of post foundations

B.1 Energy dissipation by plastic deformations of barrier posts

Energy dissipation by plastic deformations of barrier posts could be estimated based on plastic moment of the posts and the angle of rotation:

$$E = M_p \theta \qquad \text{Eq. (B1)}$$

where M_p = plastic moment of the structural member

θ = angle of rotation

M_p is the multiple of the sectional modulus (Z) and yield stress (σ_p) which equal to 22 kNm. Z and σ_p of the steel posts are 93.1 x 10^3 mm^3 and 235 MPa respectively. However, M_p is reduced to 14 kNm due to buckling failure (see M_x for Post P1 shown in Table 1). Site inspections indicated that the angle of rotation of Posts P1 and P15 was about 90^o, i.e. θ is taken as $\pi/2$. It follows that energy dissipation due to bucking of the two posts is 44 kJ for two failed posts (i.e. P1 and P15).

B.2 Energy dissipation by failure of post foundations

The energy dissipation due to foundation failure of posts relates to the sliding resistance (R_T) acting on the post foundation and the displacement of the foundation. A simplified approached is adopted in this calculation. It is assumed that R_T, which comprises the resistance acting on the base of the foundation (R_S) and the passive resistance (R_P), is constant throughout displacement process (see Figure B1).

Calculation of R_P:

$$R_P = 0.5\, k_p\, \gamma\, H^2\, w \qquad \text{Eq. (B2)}$$

where k_p is passive pressure coefficient = 3.7 (using Rankin theory with friction angle at the interface of the foundation and ground = 35^o assumed)

γ is unit weight of soil, assumed to be 18 kN/m^2

H is depth of foundation = 0.5 m

w is width of foundation = 0.4 m

Hence, R_p = 6.7 kN (say 7 kN)

Calculation of R_S:

$$R_S = N \tan \phi \qquad \text{Eq. (B3)}$$

where N is normal force acting on the base of foundation (= 68 kN), which is the calculated axial compression force when UDP = 50 kPa (see Table 1), with self-weight and side friction neglected

ϕ is friction angle at the interface of the foundation and ground = 35 ^{o} assumed

Hence, R_S = 48 kN

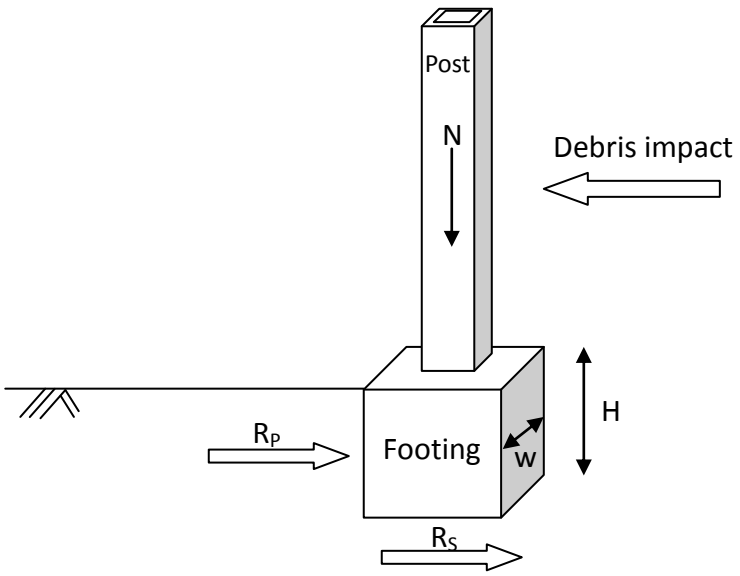

Figure B1 Calculation of the sliding resisting acting of the post foundation

Total sliding resistance, $R_T = R_S + R_P = 55$ kN

Energy dissipation is approximated by the multiple of R_T and displacement of foundations. The displacements of Posts P1 and P15 are 2.2 m and 1 m respectively as observed on site. It follows that the energy dissipation due to failure of post foundation is 176 kJ.